

7. Varilux 2, the physiological design

The background

One major characteristic element of the Varilux 1 concept was to stay close to the structure of the bifocal lens with an upper aberration free half of the surface for far vision and a rather large "segment" for clear near vision . This segment was bounded by the unavoidable aberrations which made it not always easy to get accustomed to the new lens. So in his following patents US 3 687 528 and US 3 910 691 Maitenaz described the progressive design for which the model was not the bifocal but the visual process. Introducing the evolutive conics as orthogonal sections and an orthoscopic surface structure to preserve the orientation of the horizontal and vertical object lines it was possible to reduce the aberrations and to distribute them over the surface in a way not only considering the visual acuity but also the distortion under static and dynamic viewing conditions. The result of taking into account this global character of the visual process was the creation of a totally aspheric design for Varilux 2. . The overall aspheric design of Varilux 2 was an enormous progress, it was the birth of the modern progressive lens and model for all the future lens generations .

Basic ideas

The example of the Varilux 1 design shows that surfaces composed of circles as orthogonal sections give a rather high amount of lateral aberrations.

While the astigmatism on the main meridian is zero as here the circle curvature is exactly identical with the curvature of the main meridian (umbilical line) , in the periphery this is not true anymore. In a lateral point of this circle the vertical meridian of the surface -- i.e. the intersection curve between the surface and a vertical plane containing the surface normal in this point -- is stronger curved than the circle, i.e. in this lateral point we will find surface astigmatism increasing with the distance of this point from the main meridian. We cannot eliminate these aberrations, but we can reduce them. If for such a design one of the sections is a circle, then the sections below have to be curves, whose curvature is flattening to the edge whereas the curvature of the sections above the circle is increasing with increasing x-coordinate.

In the Varilux 2 design this general principle has been realized by the concept of the evolutive conics. According to an example quoted in patent US 3 687 528 this evolution starts in the far vision portion with flattened ellipses, followed by a circle, elongated ellipses, a parabola and ending with hyperbola in the near vision portion.

This structure of the surface, built of a group of evolutive conic sections, may be considered as a first approximation. Another essential requirement for the Varilux 2 construction is the so called orthoscopy, i.e. the distortion of horizontal and vertical lines should be as small as possible.

In order to obtain good orthoscopy the patent design includes two horizontal umbilical lines at $V_z=+9^\circ$ and -12° and two vertical isoprismatic lines at $V_x=+22.5^\circ$ and -22.5° , giving a constant horizontal component of the prismatic effect.

The results of the so calculated surface are given in Fig. 22 of the patent US 3 687 528, which shows the curvatures of the orthogonal sections. In the following we will analyze the characteristic data of this design.

7.1 The Coordinate System

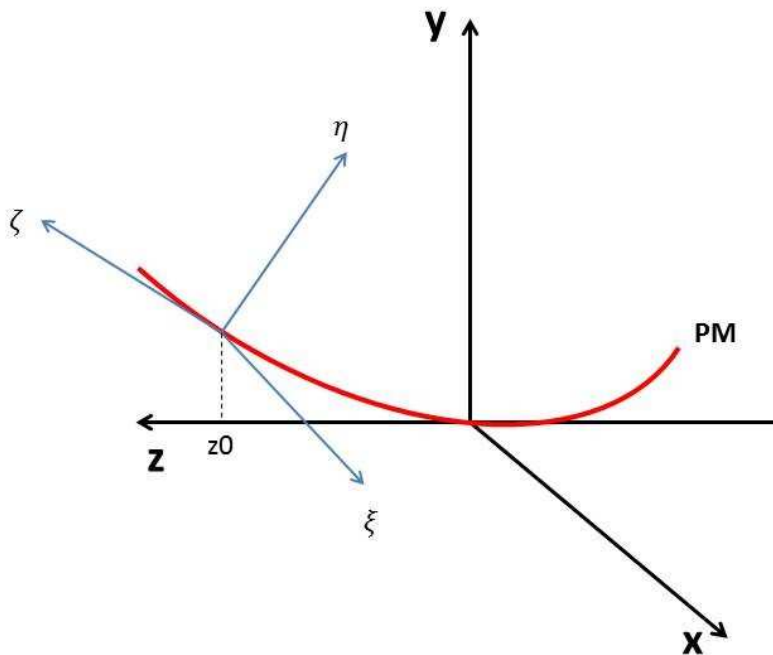


Fig 1

In Fig 1 the main meridian is situated in the yz plane of a Cartesian coordinate system (x,y,z) . Moving from near vision to far vision z increases, the z -axis being tangent to a point in between (for example the center of the finished lens where the prismatic effect is controlled). In the patent US 3 687 528 the vertical z -axis is identified with the y -coordinate.

The orthogonal sections are described in a Cartesian coordinate system (ξ,η,ζ) moving with the orthogonal section. Where the section intersects the main meridian is the origin of this coordinate system, the ζ -axis being tangent to the principal meridian, increasing ζ meaning increasing z . So in this system the orthogonal section is described by an equation between ξ and η , ξ - and x -values are identical.

7.2 The principal meridian

The table of Fig 22 of the patent gives the curvature radii of the orthogonal sections as a function of the spherical coordinates V_x and V_z (see Fig18 of the patent US 3 687 528). We will try to represent the row $V_x=0$, which is the principal meridian, by an analytical function. **All coordinates and lengths are given in mm.**

$V_z=const$ is not the condition for an orthogonal but for a horizontal section. A rough estimation shows, that the mean deviation for the curvature radius is less than 0.5 mm. So the figures of table Fig 22 have been accepted as approximation for the radii of the orthogonal sections.

Calculating the main meridian

From Fig 18 (patent) we deduce

$$z_0(V_z) := 76.80 \cdot \sin\left(V_z \cdot \frac{\pi}{180}\right)$$

Listing from Fig 22 the values of the curvature radius RM of the principal meridian together with the corresponding z_0 -values we get:

RM:=	[68.35]	Z0:=	[-27.23]	(Z0 values slightly modified to symmetrize the meridian)
	[65.88]		[-23.54]	
	[63.97]		[-19.77]	
	[63.13]		[-15.92]	
	[63.97]		[-12]	
	[65.88]		[-8.03]	
	[68.35]		[-4.02]	
	[70.30]		[-1.61]	
	[71.29]		[0]	
	[73.88]		[4.02]	
	[75.57]		[8.03]	
	[76.40]		[12.02]	
	[75.57]		[15.96]	
	[73.88]		[19.87]	
	[71.29]		[23.71]	
	[68.35]		[27.48]	

The radius of curvature has a maximum of 76.40 mm and a minimum of 63.13 mm. With an index of refraction of $n=1.525$ this corresponds to a far vision diopter of 6.9 D and an add power of 1.45 D

A cubic spline interpolation gives the function $Rm_1(z_0)$ which is graphically represented in Fig 2:

$$S := \text{cspline}(Z0, RM)$$

$$Rm1(z0) := \text{interp}(S, Z0, RM, z0)$$

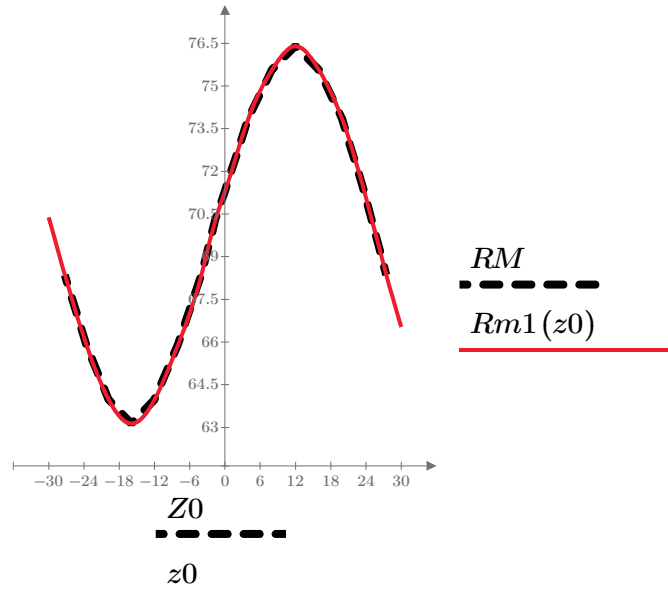
$$z0 := -30, -29.5..30$$


Fig 2

Fig 3 shows that $Rm1(z0)$ can be approximated by the following analytical sine -function

$$Rm(z0) := 69.765 + 6.635 \cdot \sin\left(\frac{2 \pi \cdot z0}{54.83} + 0.25\right)$$

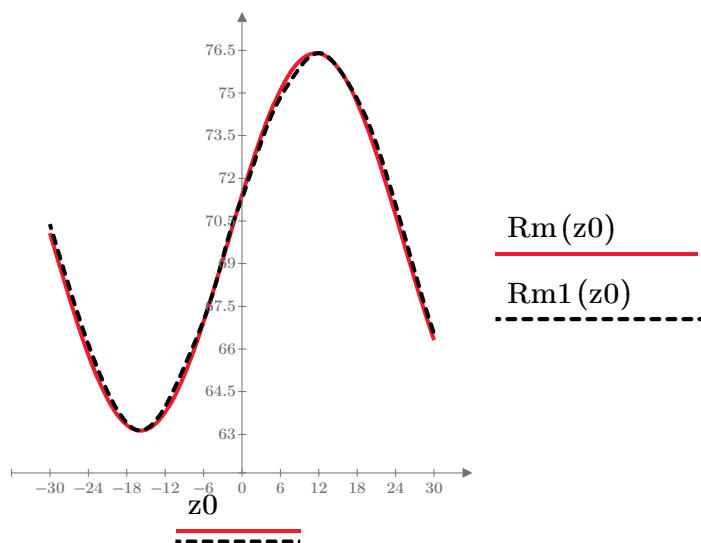
$$z0 := -27, -26..27$$


Fig 3

The tangents to the main meridian in $Vz=-12$ and $Vz=9$ are parallel to the z-axis and in the far vision part above $Vx=9$ the power increases to the top of the design and in the near vision zone below $Vx=-12$ the power decreases to the bottom of the design.

Integrating the differential equation for the curvature $K(z_0)$ of the meridian

$$\frac{Fm''(z_0)}{\left(1 + Fm'(z_0)^2\right)^{\frac{3}{2}}} = K(z_0) \quad Fm(z_0) = x_1(z_0)$$

$$x_1'(z_0) = x_2(z_0)$$

$$x_2'(z_0) = K(z_0) \cdot \left(1 + x_2(z_0)^2\right)^{\frac{3}{2}}$$

$$K(z_0) := \frac{1}{Rm(z_0)}$$

$$D(z_0, X) := \begin{bmatrix} X_1 \\ \frac{3}{2} \\ \left(1 + X_1^2\right) \cdot K(z_0) \end{bmatrix}$$

$$X(z_0) = \begin{bmatrix} x_1(z_0) \\ x_2(z_0) \end{bmatrix}$$

$$u := 6.298 \quad mm \quad v := 0.448$$

$$\text{init} := \begin{bmatrix} u \\ v \end{bmatrix}$$

u and v are the initial conditions for $Fm(z_0)$ and $D1Fm(z_0)=Fm'(z_0)$ in $z_0=30$ mm, estimated first from a circle with $rf=74$ mm (tangent to the z-axis in $z_0=0$) and then iteratively corrected, so that for $z_0=0$ $Fm(z_0)$ and $D1Fm(z_0)$ are zero

$$Z0i := 30$$

$$Z0f := -30$$

$$N := 100$$

$$\text{Sol} := \text{AdamsBDF}(\text{init}, Z0i, Z0f, N, D)$$

	$z0$	$x1 = Fm$	$x2 = Fm'(z0)$
Sol =	30	6.298	0.448
	29.4	6.033	0.436
	28.8	5.775	0.425
	28.2	5.523	0.413
	27.6	5.279	0.402
		\vdots	

Calculating the main meridian as a function of $z0$: $Fm(z0)$

arranging the data in ascending order of $z0$:

$$\text{data} := \text{csort}(\text{Sol}, 0)$$

	$z0$	$X1 = Fm(z0)$	$X2 = D1Fm(z0)$
data =	-30	7.253	-0.513
	-29.4	6.949	-0.501
	-28.8	6.652	-0.489
	-28.2	6.362	-0.477
		\vdots	

$$Z0 := \text{data}^{(0)}$$

$$X1 := \text{data}^{(1)}$$

$$X2 := \text{data}^{(2)}$$

$$S := \text{cspline}(Z0, X1)$$

$$Fm(z0) := \text{interp}(S, Z0, X1, z0)$$

$$S := \text{cspline}(Z0, X2)$$

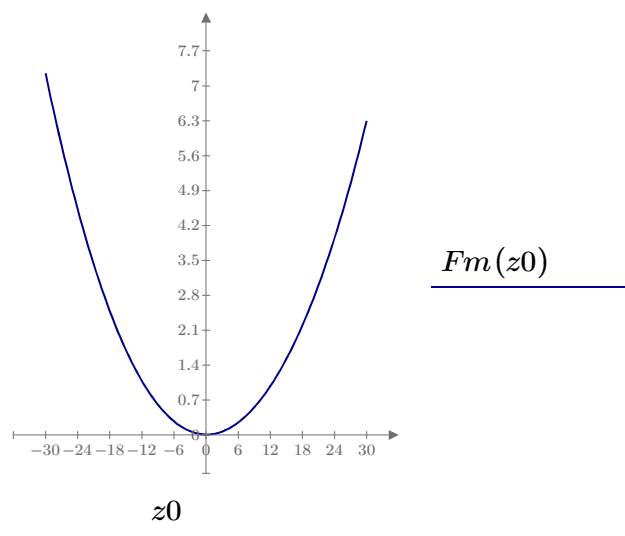
$$z0 := -30, -29.5 \dots 30$$


Fig 4

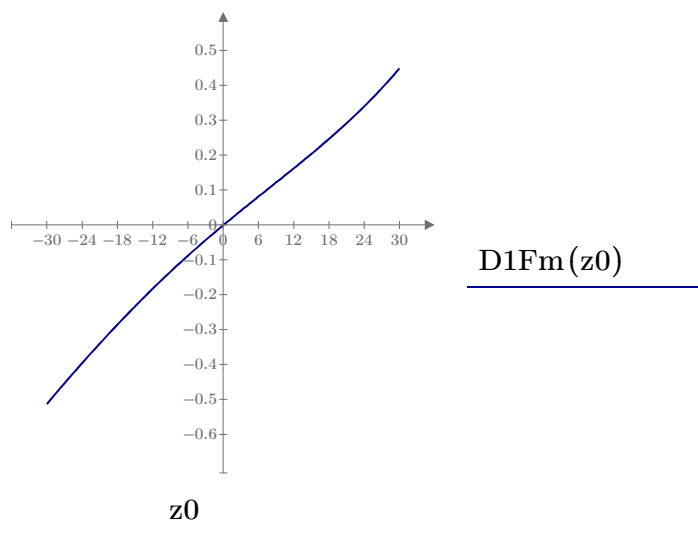
$$D1Fm(z0) := \text{interp}(S, Z0, X2, z0)$$


Fig 5

7.3 The characteristic data of the conic sections

We assume that the orthogonal sections of the Varilux 2 design are conic sections and that the principal meridian is an umbilic.

Then the vertex equation of of a conic section in the (ξ,η)-system is

$$\eta = h \cdot \left(1 - \sqrt{1 - \frac{\xi^2}{Rm \cdot h}} \right)$$

where h is the half-axis of the conic section in direction of the η -axis. $h > 0$ is an ellipse , $h < 0$ an hyperbola and $h \rightarrow \pm\infty$ means a parabola. In paragraph 7.5 we calculate the values of h for the different z_0 -values using the figures of Fig 22 (patent US 3 687 528) for the the curvature radii of the orthogonal sections. We will see that the orthogonal sections have a more complex characteristic than that of a conic section . The conic section geometry is only a first approximation which we will use in the following calculations.

In determining the conic section, we choose h so, that the curvature of the conic section and of the real orthogonal section of Fig 22 coincide for $\forall x = 15^\circ$. The calculations of h in paragraph 7.5 gives 3 zones

zone 1 for z_0 values > -13.3 : positive h-values, i.e. ellipses

zone 2 for z_0 -values between -13.3 and -18.6: negative h, hyperbola

zone 3 for z_0 -values < -18.6 : positive h, i.e. ellipses

for $z_0 = -13.3$ and $z_0 = -18.6$ there are two parabola , i.e. h is becoming infinity

zone 1: z0 > -13.3

The resulting values for the parameter h and the coordinate z0 are given in the following matrix:

```

data := [ -13.01  8000 ]
         [ -12.52  4500 ]
         [ -12.01  2650 ]
         [ -11.02  1200 ]
         [ -10.02   550 ]
         [  -9.03   271 ]
         [  -8.03   205 ]
         [  -7.03   160 ]
         [  -6.03   131 ]
         [  -5.03   109 ]
         [  -4.02   93.5 ]
         [  -1.61   70.2 ]
         [    0    59.18 ]
         [   4.02   43.73 ]
         [   8.03   37.22 ]
         [  12.01   35.72 ]
         [  15.97   37.92 ]
         [   18    41.3 ]
         [  19.88   45.28 ]
         [  23.73   61.97 ]
         [   26    85 ]
         [  27.52   97.94 ]

```

Calculation of the half-axis h1(z0) as a function of z0

$$Z0 := \text{data}^{(0)} \qquad H := \text{data}^{(1)}$$

Cubic spline interpolation

$$S := \text{cspline}(Z0, H)$$

$$h11(z0) := \text{interp}(S, Z0, H, z0)$$

$$z0 := -15, -14.5 .. 26$$

$$z0 = \begin{bmatrix} -15 \\ -14.5 \\ -14 \\ -13.5 \\ -13 \\ -12.5 \\ \vdots \end{bmatrix} \quad h11(z0) = \begin{bmatrix} 5.928 \cdot 10^4 \\ 3.883 \cdot 10^4 \\ 2.412 \cdot 10^4 \\ 1.414 \cdot 10^4 \\ 7.905 \cdot 10^3 \\ 4.4 \cdot 10^3 \\ \vdots \end{bmatrix}$$

In order to get a smooth transition until the second derivative in the range between -5 and -14 ,where the curve accelerates its growth, we insert a smoothing step

$$Z01 := \begin{bmatrix} -15 \\ -14.5 \\ -14 \\ -13.5 \\ -13 \\ -12.5 \\ -12 \\ -11.5 \\ -11 \\ \vdots \end{bmatrix} \quad H1 := \begin{bmatrix} 5.92828 \cdot 10^4 \\ 3.88307 \cdot 10^4 \\ 2.41186 \cdot 10^4 \\ 1.41442 \cdot 10^4 \\ 7.90535 \cdot 10^3 \\ 4.39968 \cdot 10^3 \\ 2.62499 \cdot 10^3 \\ 1.69794 \cdot 10^3 \\ 1.18319 \cdot 10^3 \\ \vdots \end{bmatrix}$$

$$ss1 := \text{supsmooth}(Z01, H1)$$

$$S := \text{cspline}(Z01, ss1)$$

$$h11(z0) := \text{interp}(S, Z01, ss1, z0)$$

Taking into account the symmetry around $Vz=9^\circ$, i.e. $z_0=12.01$, we obtain the half-diameter h_1 for $z_0 > -13.3$ (infinity threshold, see below)

$$h_1(z_0) := \begin{cases} h_{11}(z_0) & \text{if } z_0 \leq 12.01 \\ h_{11}(24.02 - z_0) & \text{else} \end{cases}$$

Because of the strong increase for z_0 -values below -5 we present $h_1(z_0)$ in Fig 6 and 7 with 2 different scales

$$z_0 := -3, -2.5 \dots 27$$

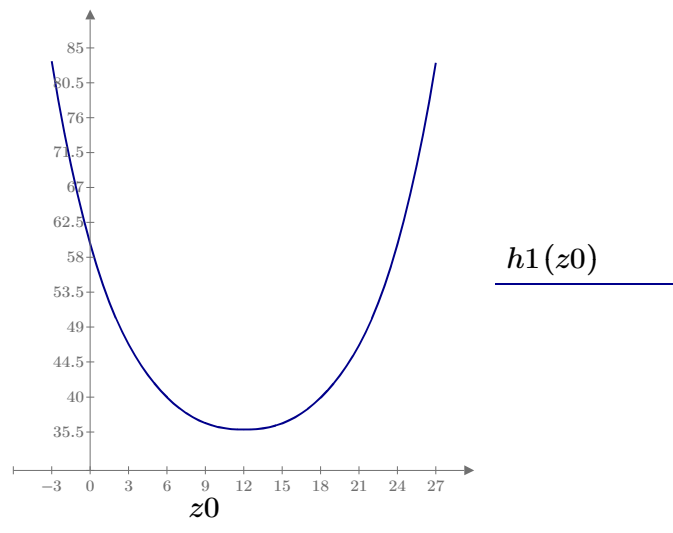


Fig 6

and compare it with the initial discrete data H of Fig 22 (patent)

$z_0 := -13, -12.5 \dots 27$

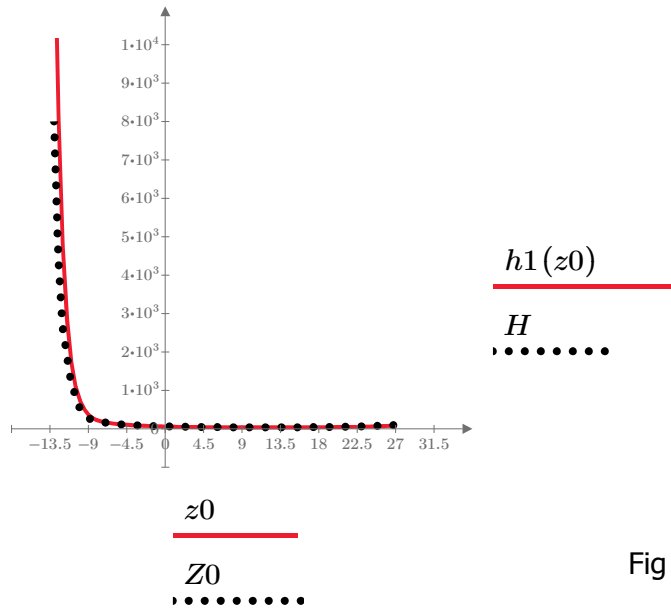


Fig 7

Where is $h_1(z_0)$ becoming infinity ?

$z_0 := -13.60, -13.50 \dots -13.00$

$$h_1(z_0) = \begin{bmatrix} 2.28 \cdot 10^4 \\ 2.103 \cdot 10^4 \\ 1.933 \cdot 10^4 \\ 1.772 \cdot 10^4 \\ 1.62 \cdot 10^4 \\ 1.476 \cdot 10^4 \\ 1.342 \cdot 10^4 \end{bmatrix} \quad z_0 = \begin{bmatrix} -13.6 \\ -13.5 \\ -13.4 \\ -13.3 \\ -13.2 \\ -13.1 \\ -13 \end{bmatrix}$$

$z_0 = -13.3$ was selected being sufficiently high to be practically infinity

zone 3: $z_0 < -18.6$ **Calculation of the half-axis $h_3(z_0)$ as a function of z_0**

As we can see from Fig 22 of the Varilux 2-patent in the lower half of the table the surface is symmetrical to the horizontal line $V_z = -12$ which corresponds to $z_0 = -15.97$. So there is a second infinity point for -18.6 and the h -values for $z_0 < -18.6$ are given by

$$h_3(z_0) := h_1(-2 \cdot 15.97 - z_0)$$

zone 2 : $-18.6 < z_0 < -13.3$

The calculations of paragraph 7.5 give the following h -values for z_0 between -18.6 and -13.3

$$\text{data} := \begin{bmatrix} -18.42 & -7862 \\ -18.19 & -4142 \\ -17.93 & -2812 \\ -16.95 & -1347 \\ -15.97 & -999 \\ -14.98 & -1316 \\ -14 & -2569 \\ -13.75 & -3547 \\ -13.50 & -5976 \end{bmatrix}$$

Calculation of the half-axis $h_2(z_0)$ as a function of z_0

$$Z_0 := \text{data}^{(0)}$$

$$H := \text{data}^{(1)}$$

cubic spline interpolation

$$S := \text{cspline}(Z_0, H)$$

$$h_{21}(z_0) := \text{interp}(S, Z_0, H, z_0)$$

taking into account the symmetry around $z_0 = -15.97$

$$h_{211}(z_0) := \frac{h_{21}(z_0) + h_{21}(-2 \cdot 15.97 - z_0)}{2}$$

Smoothing process

$$z_0 := -20.5, -20.25 \dots -11.5$$

$$h_{211}(z_0) = \begin{bmatrix} -3.648 \cdot 10^5 \\ -2.711 \cdot 10^5 \\ -1.952 \cdot 10^5 \\ -1.353 \cdot 10^5 \\ -8.949 \cdot 10^4 \\ -5.578 \cdot 10^4 \\ -3.231 \cdot 10^4 \\ -1.719 \cdot 10^4 \\ \vdots \end{bmatrix}$$

$$Z_{01} := \begin{bmatrix} -20.5 \\ -20.25 \\ -20 \\ -19.75 \\ -19.5 \\ -19.25 \\ -19 \\ \vdots \end{bmatrix} \quad H_1 := \begin{bmatrix} -(3.64785 \cdot 10^5) \\ -(2.71095 \cdot 10^5) \\ -(1.9525 \cdot 10^5) \\ -(1.35349 \cdot 10^5) \\ -(8.94921 \cdot 10^4) \\ -(5.57798 \cdot 10^4) \\ -(3.23116 \cdot 10^4) \\ \vdots \end{bmatrix}$$

$$ss2 := \text{supsmooth}(Z_{01}, H_1)$$

$$S := \text{cspline}(Z_{01}, ss2)$$

$$h_2(z_0) := \text{interp}(S, Z_{01}, ss2, z_0)$$

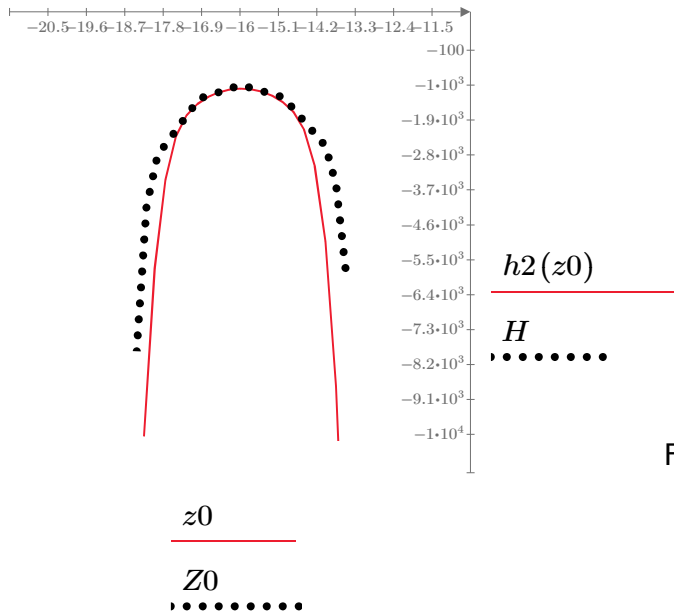


Fig 8

It was not possible to get a closer approximation of the curve to the discrete points without sacrificing a smooth second derivative in the coordinate regions near to -13.3 and -18.6.

If we now sum up the calculations for the different coordinate regions we get the following result.

The function of the half-axis $h(z_0)$ covering the whole z_0 -range between -27 and +27 mm

$$h(z_0) := \begin{cases} \text{if } z_0 > -18.6 \\ \quad \begin{cases} \text{if } z_0 > -13.3 \\ \quad h_1(z_0) \\ \quad \text{else} \\ \quad \quad h_2(z_0) \end{cases} \\ \quad \text{else} \\ \quad \quad h_3(z_0) \end{cases}$$

The graph 9 illustrates the structure of the design with evolutive conic sections, which we will discuss in detail in chapter 7.6. Fig 9a shows the upper lens portion with elliptical orthogonal sections more in detail.

$z0 := -27, -26.9..27$

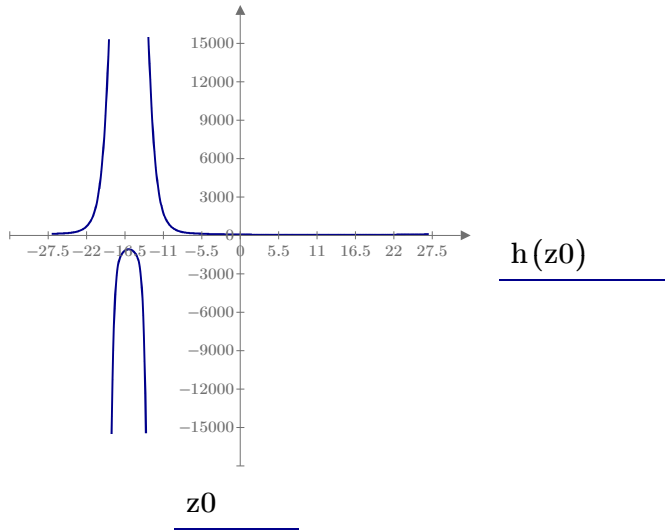


Fig 9

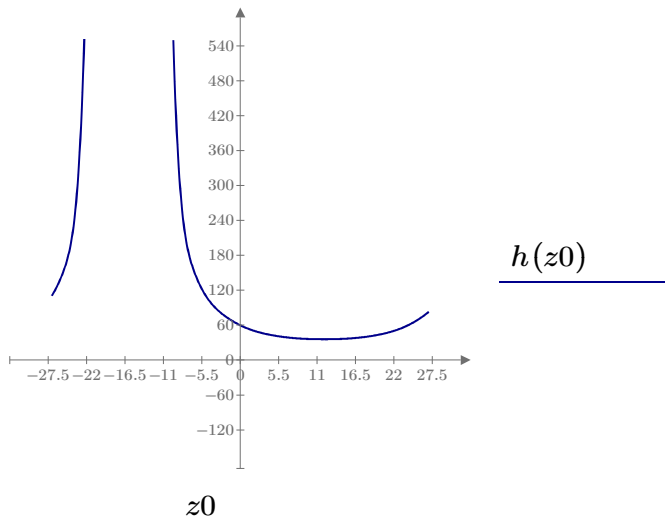


Fig 9a

7.4 Geometry and equations of the progressive surface

vertex equation of a conic section (with an umbilical main meridian)

$$\eta(z_0, \xi) := h(z_0) \left(1 - \sqrt{1 - \frac{\xi^2}{h(z_0) \cdot Rm(z_0)}} \right)$$

So in the (x, y, z) -coordinate system we get for the surface as a function of the parameter z_0, ξ

$$x(z_0, \xi) := \xi$$

$$y(z_0, \xi) := Fm(z_0) + \frac{\eta(z_0, \xi)}{\sqrt{1 + D1Fm(z_0)^2}}$$

$$z(z_0, \xi) := z_0 - \eta(z_0, \xi) \cdot \frac{D1Fm(z_0)}{\sqrt{1 + D1Fm(z_0)^2}}$$

7.4.1 Fundamental Forms

Definitions of the derivatives

$$r(z_0, \xi) := \begin{bmatrix} x(z_0, \xi) \\ y(z_0, \xi) \\ z(z_0, \xi) \end{bmatrix}$$

$$xz_0(z_0, \xi) := \frac{d}{dz_0} x(z_0, \xi)$$

$$yz_0(z_0, \xi) := \frac{d}{dz_0} y(z_0, \xi)$$

$$zz_0(z_0, \xi) := \frac{d}{dz_0} z(z_0, \xi)$$

$$r_{z0}(z_0, \xi) := \begin{bmatrix} x_{z0}(z_0, \xi) \\ y_{z0}(z_0, \xi) \\ z_{z0}(z_0, \xi) \end{bmatrix}$$

$$x_{\xi}(z_0, \xi) := \frac{d}{d\xi} x(z_0, \xi)$$

$$y_{\xi}(z_0, \xi) := \frac{d}{d\xi} y(z_0, \xi)$$

$$z_{\xi}(z_0, \xi) := \frac{d}{d\xi} z(z_0, \xi)$$

$$r_{\xi}(z_0, \xi) := \begin{bmatrix} x_{\xi}(z_0, \xi) \\ y_{\xi}(z_0, \xi) \\ z_{\xi}(z_0, \xi) \end{bmatrix}$$

$$x_{z0z0}(z_0, \xi) := \frac{d^2}{dz_0^2} x(z_0, \xi)$$

$$y_{z0z0}(z_0, \xi) := \frac{d^2}{dz_0^2} y(z_0, \xi)$$

$$z_{z0z0}(z_0, \xi) := \frac{d^2}{dz_0^2} z(z_0, \xi)$$

$$r_{z0z0}(z_0, \xi) := \begin{bmatrix} x_{z0z0}(z_0, \xi) \\ y_{z0z0}(z_0, \xi) \\ z_{z0z0}(z_0, \xi) \end{bmatrix}$$

$$x_{\xi\xi}(z_0, \xi) := \frac{d^2}{d\xi^2} x(z_0, \xi)$$

$$y_{\xi\xi}(z_0, \xi) := \frac{d^2}{d\xi^2} y(z_0, \xi)$$

$$z_{\xi\xi}(z_0, \xi) := \frac{d^2}{d\xi^2} z(z_0, \xi)$$

$$\mathbf{r}_{\xi\xi}(z_0, \xi) := \begin{bmatrix} x_{\xi\xi}(z_0, \xi) \\ y_{\xi\xi}(z_0, \xi) \\ z_{\xi\xi}(z_0, \xi) \end{bmatrix}$$

$$x_{z_0\xi}(z_0, \xi) := \frac{d}{d\xi} \left(\frac{d}{dz_0} x(z_0, \xi) \right)$$

$$y_{z_0\xi}(z_0, \xi) := \frac{d}{d\xi} \left(\frac{d}{dz_0} y(z_0, \xi) \right)$$

$$z_{z_0\xi}(z_0, \xi) := \frac{d}{d\xi} \left(\frac{d}{dz_0} z(z_0, \xi) \right)$$

$$\mathbf{r}_{z_0\xi}(z_0, \xi) := \begin{bmatrix} x_{z_0\xi}(z_0, \xi) \\ y_{z_0\xi}(z_0, \xi) \\ z_{z_0\xi}(z_0, \xi) \end{bmatrix}$$

1. Fundamental Form and unit normal vector

$$E(z_0, \xi) := \mathbf{r}_{z_0}(z_0, \xi) \cdot \mathbf{r}_{z_0}(z_0, \xi)$$

$$F(z_0, \xi) := \mathbf{r}_{z_0}(z_0, \xi) \cdot \mathbf{r}_{\xi}(z_0, \xi)$$

$$G(z_0, \xi) := \mathbf{r}_{\xi}(z_0, \xi) \cdot \mathbf{r}_{\xi}(z_0, \xi)$$

$$\mathbf{N}_0(z_0, \xi) := \frac{\mathbf{r}_{z_0}(z_0, \xi) \times \mathbf{r}_{\xi}(z_0, \xi)}{\|\mathbf{r}_{z_0}(z_0, \xi) \times \mathbf{r}_{\xi}(z_0, \xi)\|}$$

2. Fundamental Form

$$L(z_0, \xi) := r_{z_0 z_0}(z_0, \xi) \cdot N_0(z_0, \xi)$$

$$M(z_0, \xi) := r_{z_0 \xi}(z_0, \xi) \cdot N_0(z_0, \xi)$$

$$N(z_0, \xi) := r_{\xi \xi}(z_0, \xi) \cdot N_0(z_0, \xi)$$

$$H1(z_0, \xi) := E(z_0, \xi) \cdot N(z_0, \xi) + G(z_0, \xi) \cdot L(z_0, \xi) - 2 \cdot F(z_0, \xi) \cdot M(z_0, \xi)$$

$$H2(z_0, \xi) := E(z_0, \xi) \cdot G(z_0, \xi) - F(z_0, \xi)^2$$

$$H3(z_0, \xi) := L(z_0, \xi) \cdot N(z_0, \xi) - M(z_0, \xi)^2$$

Principal curvatures

$$K1(z_0, \xi) := \frac{\left(H1(z_0, \xi) + \sqrt{H1(z_0, \xi)^2 - 4 \cdot H2(z_0, \xi) \cdot H3(z_0, \xi)} \right)}{2 \cdot H2(z_0, \xi)}$$

$$K2(z_0, \xi) := \frac{\left(H1(z_0, \xi) - \sqrt{H1(z_0, \xi)^2 - 4 \cdot H2(z_0, \xi) \cdot H3(z_0, \xi)} \right)}{2 \cdot H2(z_0, \xi)}$$

7.4.2 Mean optical power POW and Astigmatism AST

$$POW(z_0, \xi) := 525 \cdot \frac{(K1(z_0, \xi) + K2(z_0, \xi))}{2}$$

$$AST(z_0, \xi) := 525 \cdot (K1(z_0, \xi) - K2(z_0, \xi))$$

Check, that the principal meridian is an umbilical line

$$\xi := 0 \quad z0 := -25, -20..25$$

$$\text{AST}(z0, \xi) = \begin{bmatrix} 0.00051 \\ 0.00005 \\ 0.00018 \\ 0.0002 \\ 0.00046 \\ 0.00017 \\ 0.00009 \\ 0.00063 \\ 0.00001 \\ 0.00026 \\ 0.00008 \end{bmatrix}$$

We see that, as expected, the astigmatism on the main meridian is very small, everywhere at least less than 0.001 D

Lines of constant mean optical power (Isopower plot)

Loop calculation

$$\xi_{\min} := -24 \quad \xi_{\max} := 24 \quad n := 22 \quad i := 0..n$$

$$\Delta\xi := \frac{\xi_{\max} - \xi_{\min}}{n} \quad \xi_i := \xi_{\min} + i \cdot \Delta\xi$$

$$z0_{\min} := -24 \quad z0_{\max} := 24$$

$$\Delta z0 := \frac{z0_{\max} - z0_{\min}}{n} \quad z0_i := z0_{\min} + i \cdot \Delta z0$$

```

MPOW( $\xi, z0$ ) := || for i  $\in$  0 .. last( $\xi$ )
|| || for j  $\in$  0 .. last( $z0$ )
|| || || MPowi,j  $\leftarrow$  POW( $z0_j, \xi_i$ )
|| || || Mzi,j  $\leftarrow$  z0j
|| || || Mxi,j  $\leftarrow$  x( $z0_j, \xi_i$ )
|| || ||
|| || || [ Mx ]
|| || || [ Mz ]
|| || || [ MPow ]
|| || ||
|| return

```

$$\text{ISOPOW} := \text{MPOW}(\xi, z0) = \begin{bmatrix} [23 \times 23] \\ [23 \times 23] \\ [23 \times 23] \end{bmatrix}$$

Mathcad program

$$\text{FA}(\xi, z0) := \text{POW}(z0, \xi)$$

$$\xi_{\text{low}} := -24 \quad \xi_{\text{high}} := 24 \quad \xi_n := 23$$

$$z0_{\text{low}} := -24 \quad z0_{\text{high}} := 24 \quad z0_n := 23$$

$$\text{FA} := \text{CreateMesh}(\text{FA}, \xi_{\text{low}}, \xi_{\text{high}}, z0_{\text{low}}, z0_{\text{high}}, \xi_n, z0_n)$$

In order to interpret the isopower lines correctly remember that the far vision power is 6.9 D and the Add 1.45 D.

Fig 10 shows the general structure of the isopowerlines in steps of 0.5 D. The isopower-plot in 0.125 steps (Fig 10a) shows the add power increase in detail and will help us to determine the length of the power progression.

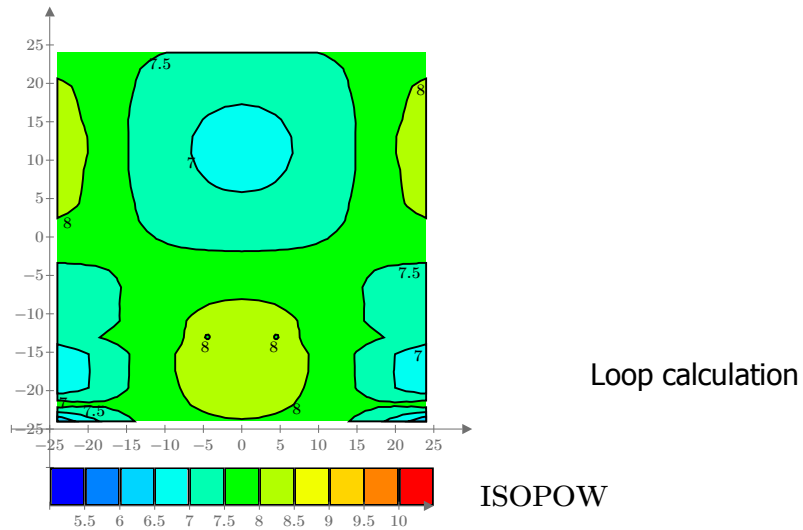
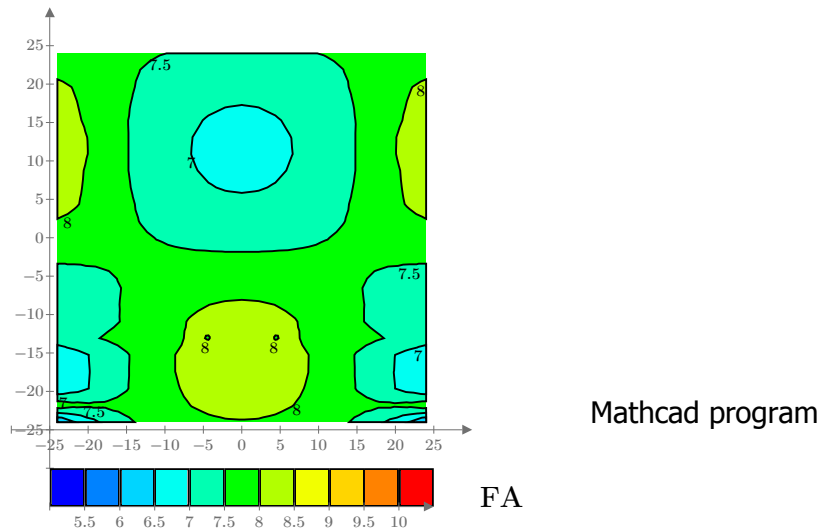


Fig 10



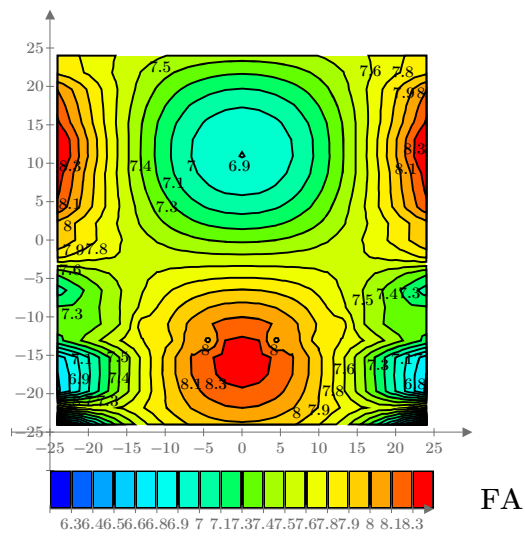


Fig 10 a

Lines of constant astigmatism (Isoastigmatism plot)

Loop calculation

$$\xi_{\min} := -24 \quad \xi_{\max} := 24 \quad n := 22 \quad i := 0..n$$

$$\Delta\xi := \frac{\xi_{\max} - \xi_{\min}}{n} \quad \xi_i := \xi_{\min} + i \cdot \Delta\xi$$

$$z_{0\min} := -24 \quad z_{0\max} := 24$$

$$\Delta z_0 := \frac{z_{0\max} - z_{0\min}}{n} \quad z_{0_i} := z_{0\min} + i \cdot \Delta z_0$$


```

MAST( $\xi, z0$ ) := || for i  $\in$  0 .. last( $\xi$ )
|| || for j  $\in$  0 .. last( $z0$ )
|| || || MAstii,j  $\leftarrow$  AST( $z0_j, \xi_i$ ) - 0.1
|| || || Mzi,j  $\leftarrow$  z0j
|| || || Mxi,j  $\leftarrow$  x( $z0_j, \xi_i$ )
|| || ||
|| || || [ Mx ]
|| || || [ Mz ]
|| || || [ MAsti ]
|| return

```

(In order to see the characteristics of the design better for low astigmatism values (particularly for the two horizontal umbilical lines) we shifted the zero point by 0.1 D to the right).

$$\text{ISOAST} := \text{MAST}(\xi, z0) = \begin{bmatrix} [23 \times 23] \\ [23 \times 23] \\ [23 \times 23] \end{bmatrix}$$

Mathcad program

$$\text{FA}(\xi, z0) := \text{AST}(z0, \xi) - 0.1$$

$$\xi_{\text{low}} := -24 \quad \xi_{\text{high}} := 24 \quad \xi_n := 23$$

$$z0_{\text{low}} := -24 \quad z0_{\text{high}} := 24 \quad z0_n := 23$$

$$\text{FA} := \text{CreateMesh}(\text{FA}, \xi_{\text{low}}, \xi_{\text{high}}, z0_{\text{low}}, z0_{\text{high}}, \xi_n, z0_n)$$

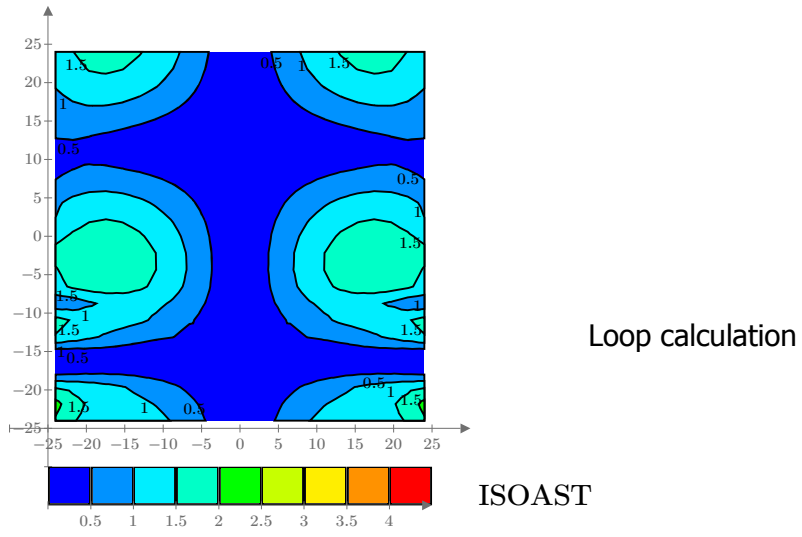
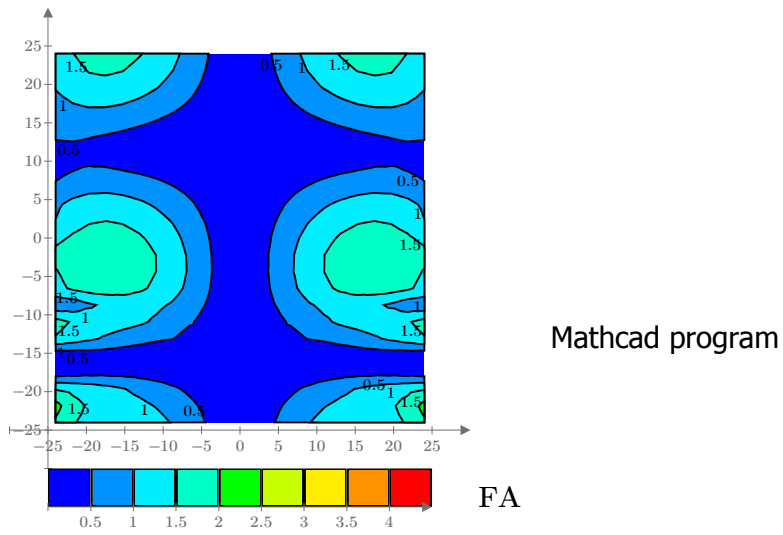


Fig 11



7.5 Calculation of the half-axis $h(z_0)$ of the conic sections (according to table fig 22 of patent US 3 687 528)

In table fig 22 of the patent the radii of the orthogonal sections, which (in a first approximation) we assume to be conical sections, are given for different V_x - and V_z -values. So we will introduce for the following calculation V_x and V_z as the independent variables in the equations for the conic sections

$$\xi(V_x) := 76.80 \cdot \sin\left(V_x \cdot \frac{\pi}{180}\right) \quad z_0(V_z) := 76.80 \cdot \sin\left(V_z \cdot \frac{\pi}{180}\right)$$

$$\eta(V_z, V_x) := h(z_0(V_z)) \left(1 - \sqrt{1 - \frac{\xi(V_x)^2}{h(z_0(V_z)) \cdot R_m(z_0(V_z))}} \right)$$

$$\eta\xi(V_z, V_x) := \frac{\frac{d}{dV_x} \eta(V_z, V_x)}{\frac{d}{dV_x} \xi(V_x)} \quad \eta\xi\xi(V_z, V_x) := \frac{\frac{d}{dV_x} \eta\xi(V_z, V_x)}{\frac{d}{dV_x} \xi(V_x)}$$

The orthogonal section has then the radius of curvature :

$$\rho(V_z, V_x) := \left(\frac{\eta\xi\xi(V_z, V_x)}{\left(1 + \eta\xi(V_z, V_x)\right)^{\frac{3}{2}}} \right)^{-1}$$

If we want to approximate the sections $V_z = \text{const}$ in Fig 22 by conic sections, we have to choose a specific value of V_x , called V_{xr} , where the radius of curvature ρ is identical with the curvature value in Fig 22. We will call this radius of curvature $\rho(V_z, V_{xr}) = \rho_0(V_z)$ and choose $V_{xr} = 15^\circ$. Compared with other tested values, $V_{xr} = 6$ and $V_{xr} = 9$, the fitting between numerical values of the table and the calculated conic section is the best. The half-Axis H (see paragraph 7.3) in the direction of the η -axis is given by the expression:

$$H(V_z, V_{xr}, \rho_0) := Rm(z_0(V_z)) \cdot \frac{\xi(V_{xr})^2}{\xi(V_{xr})^2 - Rm(z_0(V_z))^2 \cdot \left(\left(\frac{\rho_0}{Rm(z_0(V_z))} \right)^{\frac{2}{3}} - 1 \right)}$$

In the following we calculate H for the different orthogonal sections $V_z = -21^\circ$ to $V_z = 21^\circ$. For the sections $V_z = +/- 21^\circ$ and $+/- 18^\circ$ where in table Fig 22 there are no ρ_0 -values for $V_{xr} = 15^\circ$ we take the $V_{xr} = 15^\circ$ values for $V_z = -3^\circ$ and -6° respectively (surface symmetry).

Generally holds :

$$V_{xr} := 15 \quad \xi(V_{xr}) = 19.88$$

The results for the different V_z are :

$$V_z := -21 \quad z_0(V_z) = -27.52 \quad Rm(z_0(V_z)) = 68.2 \quad \rho_0 := 70.72$$

$$H(V_z, V_{xr}, \rho_0) = 95.78$$

$$V_z := -18 \quad z_0(V_z) = -23.73 \quad Rm(z_0(V_z)) = 65.63 \quad \rho_0 := 71.87$$

$$H(V_z, V_{xr}, \rho_0) = 205.15$$

$$V_z := -15 \quad z_0(V_z) = -19.88 \quad Rm(z_0(V_z)) = 63.81 \quad \rho_0 := 72.86$$

$$H(V_z, V_{xr}, \rho_0) = 1346.59$$

$$V_z := -12 \quad H(V_z, V_{xr}, \rho_0) = -5506.66$$

$$V_z := -9 \quad H(V_z, V_{xr}, \rho_0) = 1446.1$$

$$V_z := -6 \quad H(V_z, V_{xr}, \rho_0) = 305.58$$

$$V_z := -3 \quad H(V_z, V_{xr}, \rho_0) = 140.01$$

$$V_z := -1.2 \quad z_0(V_z) = -1.608 \quad Rm(z_0(V_z)) = 70.201 \quad \rho_0 := 70.20$$

$$H(V_z, V_{xr}, \rho_0) = 70.2$$

$$V_z := 0 \quad H(V_z, V_{xr}, \rho_0) = 62.32$$

$$V_z := 3 \quad H(V_z, V_{xr}, \rho_0) = 49.69$$

$$V_z := 6 \quad H(V_z, V_{xr}, \rho_0) = 43.71$$

$$V_z := 9 \quad H(V_z, V_{xr}, \rho_0) = 42.23$$

$$V_z := 12 \quad H(V_z, V_{xr}, \rho_0) = 44.67$$

$$V_z := 15 \quad H(V_z, V_{xr}, \rho_0) = 51.68$$

$$V_z := 18 \quad H(V_z, V_{xr}, \rho_0) = 65.41$$

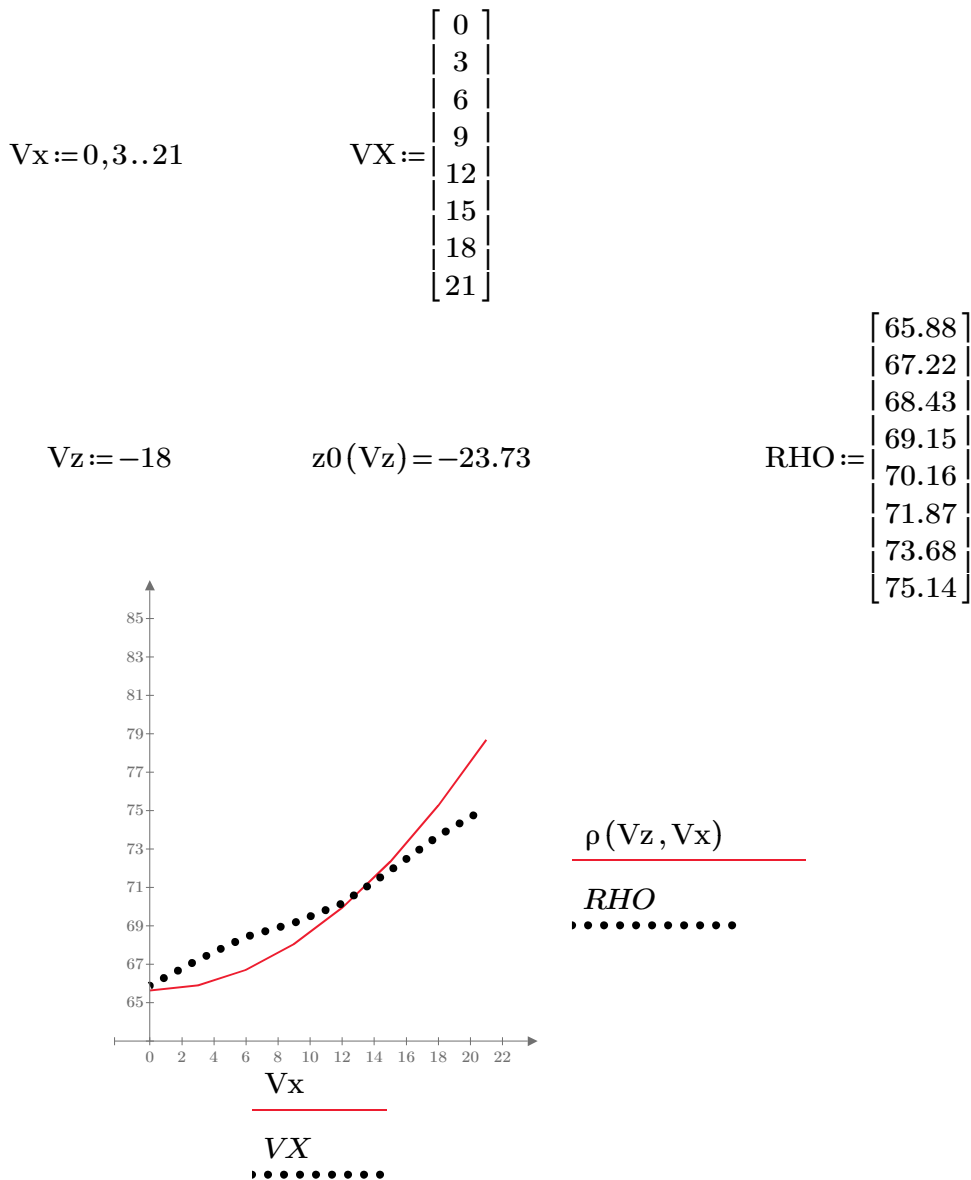
$$V_z := 21 \quad H(V_z, V_{xr}, \rho_0) = 90.27$$

7.6 Analysis of design and calculation

7.6.1 Are the orthogonal sections conics ?

One essential progress of the V2- invention is the fact, that the orthogonal sections are no circles anymore, but curves whose curvature is changing from the vertical meridian to the periphery . In the near vision part the curvature of the sections is thereby decreasing with increasing distance from the meridian and increasing in the far vision .

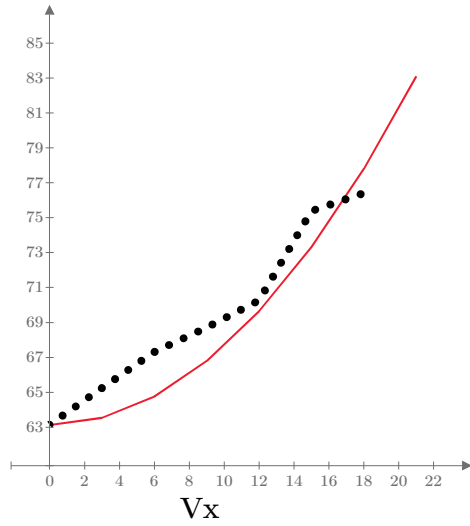
Let us now analyze how good the calculated conic sections approximate the figures of table fig 22 . We consider the table rows Vz=-18°, -12°, 0°, 9° and 18°. ρ is the curvature radius of the calculated orthogonal section section while, RHO are the values from table Fig 22



$V_z := -12$

$z_0(V_z) = -15.97$

$$RHO := \begin{bmatrix} 63.13 \\ 65.23 \\ 67.30 \\ 68.70 \\ 70.25 \\ 75.37 \\ 76.40 \end{bmatrix}$$



$$\frac{\rho(V_z, V_x)}{RHO}$$

, ,

Vx

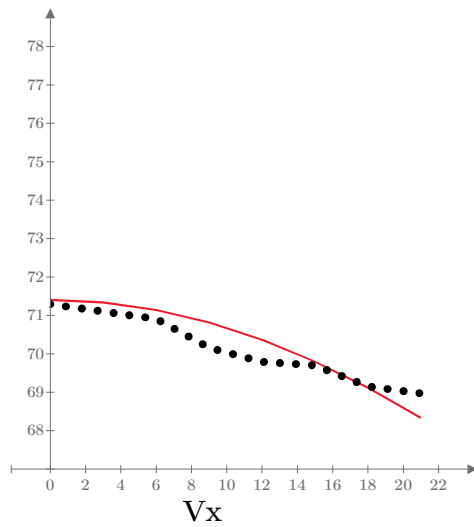
VX

, ,

$V_z := 0$

$z_0(V_z) = 0$

$$RHO := \begin{bmatrix} 71.29 \\ 71.10 \\ 70.91 \\ 70.16 \\ 69.79 \\ 69.70 \\ 69.15 \\ 68.97 \end{bmatrix}$$



$$\frac{\rho(V_z, V_x)}{RHO}$$

, ,

Vx

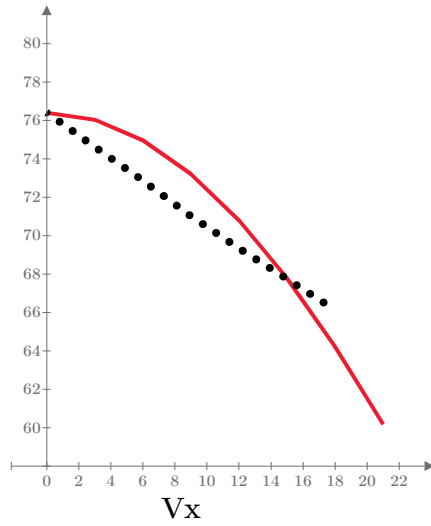
VX

, ,

$V_z := 9$

$z_0(V_z) = 12.01$

$RHO := \begin{bmatrix} 76.40 \\ 74.61 \\ 72.86 \\ 71.01 \\ 69.33 \\ 67.73 \\ 66.12 \end{bmatrix}$



$\rho(V_z, V_x)$

RHO
 ,.....

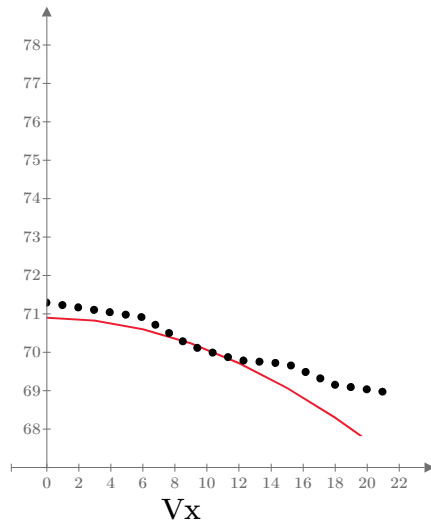
V_x

VX
 ,.....

$V_z := 18$

$z_0(V_z) = 23.73$

$RHO := \begin{bmatrix} 71.29 \\ 71.10 \\ 70.91 \\ 70.16 \\ 69.79 \\ 69.70 \\ 69.15 \\ 68.97 \end{bmatrix}$



$\rho(V_z, V_x)$

RHO
 ,.....

V_x

VX
 ,.....

The orthogonal sections of Fig 22 (patent) are no exact conics as it is also mentioned in the patent. The increase or decrease of the curvature radius from the principal meridian to the periphery in a first rough approximation is nearly linear, particularly obvious for $V_z=9$. In a second approximation we see the superposition of a sine-like modulation.

Notwithstanding in our calculations we have maintained the model of the evolutive conic sections. Consequently the results cannot reproduce exactly the results of the patent but we will see that the characteristic design features can nevertheless be demonstrated.

7.6.2 The evolutive conic sections

If we consider the approximation by conics having exactly the same curvature for $V_x = 15^\circ$ as the sections of Fig 22 of the patent, we get for the half axes of the conic sections $h(z_0)$ the results of fig 9 and fig 9a.

In these two graphs we see an evolution of the type of conical section along the meridian. Starting upwards from $V_z = -12^\circ$, i.e. the meridian point with the steepest curvature, the sections are at first hyperbola ($h < 0$) until $z_0 = -13.3$, where the section becomes a parabola. Moving further to positive z_0 -values we find elongated ellipses until $V_z = -1.15^\circ$, i.e. $z_0 = -1.54$, where we have a circle

$$V_z := -1.15$$

$$z_0(V_z) = -1.541$$

$$\rho(V_z, V_x) = \begin{bmatrix} 70.251 \\ 70.251 \\ 70.251 \\ 70.251 \\ 70.251 \\ 70.251 \\ 70.251 \\ 70.251 \end{bmatrix}$$

After the circle the sections in the FV part become oblate ellipses. Going downwards from $V_z = -12^\circ$ the sections start with hyperbolas, then a parabola at $z_0 = -18.6$ followed by elongated ellipses.

As we know, the surface is symmetrical to the horizontals $V_z = -12^\circ$ and $V_z = 9^\circ$. Thus we should expect other circles for $V_z = -22.8^\circ$ which is outside of the considered range and $V_z = 19.2^\circ$. For $V_z = 19.372^\circ$ we find an exact circle:

$$V_z := 19.372 \qquad z_0(V_z) = 25.475$$

$$\rho(V_z, V_x) = \begin{bmatrix} 69.582 \\ 69.582 \\ 69.582 \\ 69.582 \\ 69.582 \\ 69.582 \\ 69.582 \\ 69.581 \end{bmatrix}$$

The reason for the small deviations of the V_z coordinate and the radius from the circle-values of the patent is the analytical approximation of the meridian in 7.2.

7.6.3 Secondary umbilical lines

One reason that the orthogonal sections are no exact conics was the intention to reduce the distortion of horizontal and vertical lines to a maximum. Bernard Maitenaz achieved this goal in introducing isoprismatic lines in the lens design.

Horizontal lines with a constant vertical component of the prismatic effect are maintaining the orientation of horizontal lines, while a vertical line with constant horizontal components of the prismatic effect correct the distortion of verticals. The lines with constant vertical deflection have been executed as two secondary umbilics positioned at the FV reference point $V_x = 9^\circ$ and at the NV reference point $V_x = -16^\circ$, the isoprismatic lines for the horizontal component have been placed symmetrically at $V_x \pm 22.5^\circ$. We will discuss the properties of this geometry later in the chapter "Orthoscopy" (chapter 8).

7.6.4 Astigmatism-and power characteristics

The fact that the lines with constant vertical prismatic effect have been designed as horizontal umbilics can be identified in Fig 3, showing the main meridian, and in Fig 11, the Isoastigmatism plot.

In order to construct a horizontal umbilical line in a point of the vertical principal meridian and perpendicular to this meridian, the principal meridian has to reach a maximum or a minimum of curvature in the points of intersection. Thus figure 3 shows a graph of the main meridian curvature with horizontal tangents for $V_z = -12^\circ$ and $V_z = 9^\circ$. Studying the Isoastigmatism plots we see that the zones exempt from aberrations are centered around the lines $V_z = -12^\circ$ and $V_z = 9^\circ$, where the secondary umbilics have been positioned .

The astigmatism maximum is with 1.5 D , i.e. about the value of the add power and thereby neatly lower than the peripheral astigmatism of the relatively "hard" Varilux 1 design, with values of 3 x add power and more. So Varilux 2 represented an enormous progress for the adaptation and the visual comfort of progressive lenses for the wearer.

According to Figure 10 a the effective length of the power progression of the patent design is about 18 mm, if we define it by the distance of the two points on the meridian with ((FV-power +0.12 D) and (NV-power -0.12 D)). The length of the power increase for Varilux 1 add 2 is about 12 to 14 mm. Besides the optical modulation by the evolutive conics, the longer progression is an additional feature why the design of the V2-patent is much softer than the V1 type -design.

If we have a look on the figures 10 and 10 a , we notice a soft and continuous power increase in the central part and two symmetrically situated pairs of "islands" in the periphery. One "island" pair represents a power increase in the lateral upper part of the progression. The other " island" pair is the result of a power decrease in the lateral lower part of the progression. Typical for the design in the patent is the inversion of the power change above the far vision- and below the near vision- reference point.

7.6.5 Varilux 2 on the market

Was the lens sold under the brandname Varilux 2 identical with the lens design specified in the patent ?

In the patent US 4 315 673 Fig 8 b represents the average of several measurements of Varilux 2 lenses for the add 3 . As the peripheral astigmatism is roughly proportional to the add power (for mono-design lenses), we divide the astigmatism figures given in Fig 8 b by two and get a rough approximation for the astigmatism pattern of a commercial Varilux 2 for add 1.5 (Fig 12 below).

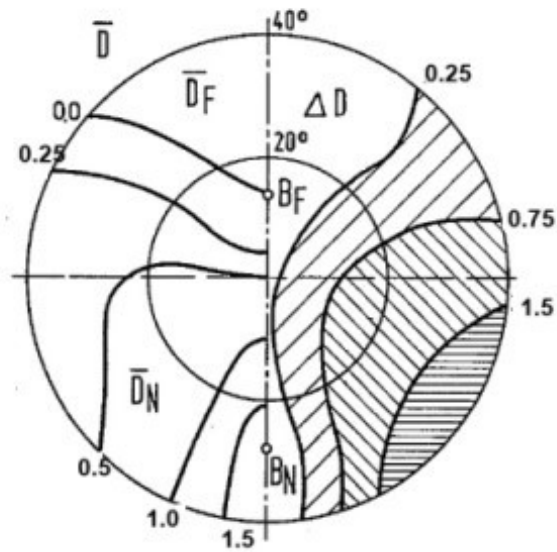


Fig 12

Even if we take into account that the manufacturing process will change the structure of the theoretical design, it is highly probable, that the measured lens has not exactly the design given in the Varilux 2 patent.

The symmetry in the design with respect to the 2 horizontals in the FV- and NV-part does not exist anymore. It is difficult to measure the effective progression length in the graph of figure 12, but it is certainly shorter than in the patent. In the near vision part the power stabilizes about 3 mm above the near vision reference point BN and above the far vision point BF the power decrease of the patent is replaced by a substantially stabilized zone. As in the patent the maximum value of the astigmatism is about 1.5 D and the aberrations extend into the lateral FV zone .